

The Effect of Tropospheric Temperature Lapse Rates on the Ascent Rates of Pilot Balloons¹

JOEY F. BOATMAN

North American Weather Consultants, Santa Barbara Municipal Airport, Goleta, Calif. 93017

11 October 1973 and 24 July 1974

ABSTRACT

By utilizing a double-theodolite tracking system in conjunction with aircraft soundings and rawinsonde observations during pilot balloon release, it was found that temperature lapse rate may have a definite and sometimes adverse effect on the ascent rates of spherical meteorological pilot balloons. An alternative to the common usage of assumed ascent rates is proposed for common environmental temperature lapse rates.

1. Introduction

The height of a pilot balloon depends on the reliability of the assumed ascent rate of the balloon when using a single-theodolite system. Since it was desirable to have considerable precision in our measurements of the wind fields over St. Louis,² it was decided to make several double-theodolite system releases with the intent of determining the best rise rate V for our single-theodolite work.

Upon computer reduction of these double-theodolite data, it was found that in one case the pilot balloon seemed to cease rising at a certain altitude in the atmosphere and in another the pilot balloon had a more constant rise rate. A comparison of these balloon ascension rates with aircraft soundings and regional National Weather Service (NWS) rawinsonde releases revealed that the temperature lapse rate seemingly had a definite effect on balloon rise rate.

Other limited examples of the effect of temperature lapse rate on the ascensional rates of pilot balloons have been cited by Reynolds (1966), Baynton (1968), Butler and Duncan (1968), and Rider and Armendariz (1970). While these researchers suggest temperature vs ascensional rate relationships, their full significance has not yet been documented. For this reason, it was decided to expand the scope of pilot balloon observations with the hope of sorting out some consistency in ascent rate as a function of temperature lapse rate.

2. Procedures

For this study, over 50 pilot balloons were released principally in the vicinity of Laramie, Wyo. Pilot

balloon releases consisted of both 30- and 100-gm spherical neoprene balloons of various colors (white, red and black—identical to those used by the NWS) inflated with helium. The smaller balloons were filled until a free lift of 125 gm was attained (i.e., the balloon was neutrally buoyant with 125 gm of mass attached), while a free lift of 250 or 445 gm was used with the larger balloons. It should be noted here that the NWS uses 139 and 449 gm of free lift, respectively, with the 30- and 100-gm pilot balloons.

Filling procedures for our pilot balloons were essentially identical to those of the NWS. A precision-machined weight was used as a filling nozzle and attached to a helium supply by a 22-inch Tygon tube. The inflation began when a pilot balloon was attached to the nozzle weight. When the pilot balloon, nozzle weight, and Tygon tube system became neutrally buoyant, filling was complete. During cold weather launches, all pilot balloons were preheated, as the NWS recommends.

In our double-theodolite launches, the two tracking theodolites were separated by a base leg of 1000 ft, carefully measured to within ± 1 ft. Checks of theodolite balance and orientation were also routinely made before and after each launch. Data obtained from double-theodolite tracks were then reduced by computer using the trigonometric calculations outlined in Circular O (U. S. Weather Bureau, 1942).

This double-theodolite data reduction scheme was verified by calculating the heights of various known elevations on two radio towers. Comparisons between the actual and computed heights of radio tower sections appear in Table 1. It can be seen from these results that the actual error did not exceed the maximum theoretical relative error in this controlled test.

¹ Work performed while the author was a graduate research assistant at the University of Wyoming, Laramie.

² Site of Project METROMEX, August 1971–72.

TABLE 1. Comparison between actual and computed heights of structural sections of two radio towers.

Case I			
Actual height (ft)	Computed height (ft)	Actual error (%)	Theoretical relative error (%)
63.00	61.40	2.59	3.28
108.00	107.02	0.90	1.74
153.00	152.92	0.05	1.20
198.00	196.85	0.58	0.90
243.00	243.60	0.24	0.75
288.00	288.58	0.20	0.63
333.00	334.21	0.36	0.54
378.00	378.18	0.05	0.48
468.00	468.63	0.01	0.40
513.00	515.38	0.05	0.37

Case II			
Actual height (ft)	Computed height (ft)	Actual error (%)	Theoretical relative error (%)
81.00	81.00	0.74	2.48
150.00	150.00	0.00	1.28
219.00	271.60	0.63	0.87
288.00	288.80	0.28	0.59
357.00	356.46	0.15	0.53
426.00	425.79	0.05	0.45
476.00	473.16	0.06	0.41

Launch days were chosen on the basis of analysis of temperature lapse rates obtained from rawinsonde

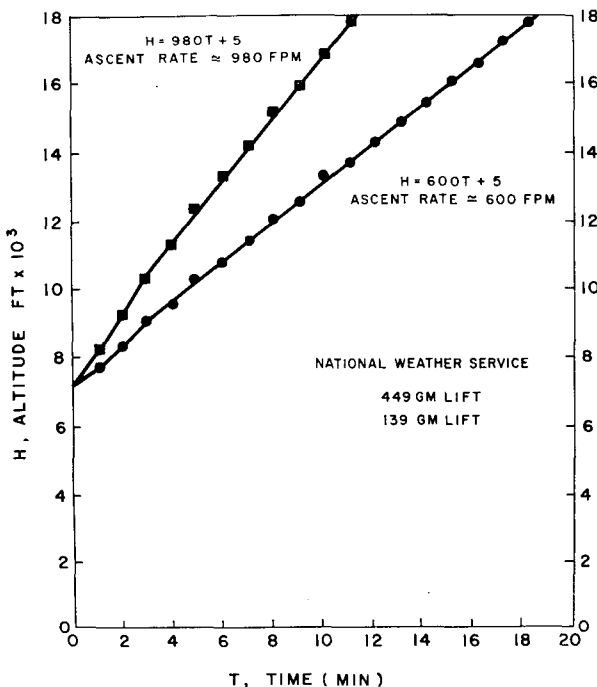


FIG. 1. Height vs time plot assumed by the National Weather Service for its 139-gm and 449-gm free-lift balloons in all atmospheric conditions. Best-fit equations are also shown for both balloon types with their respective derived ascent rates.

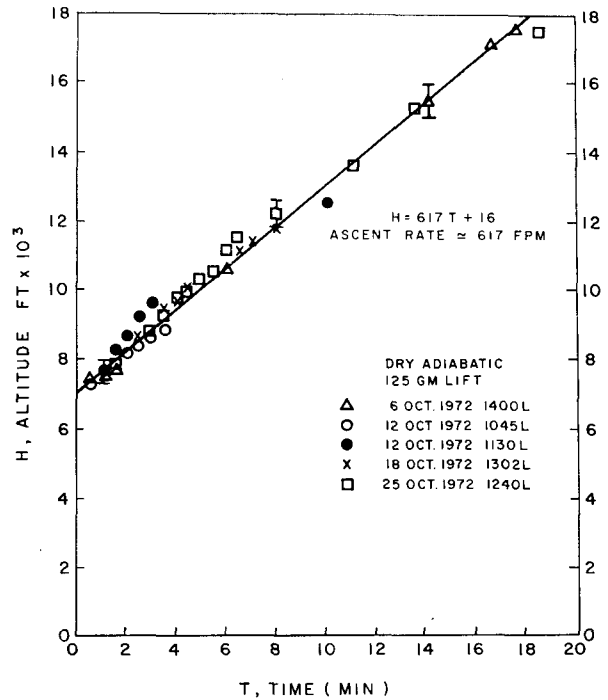


FIG. 2. Composite height vs time plot for 30-gm (125 gm free-lift) balloons rising through a dry adiabatic environment from the surface. A best-fit equation is shown with resulting derived balloon ascent rate. Error bars delineate expected accuracy of the measurements.

releases by appropriate regional NWS observing stations. Special emphasis was placed on days with deep dry or moist adiabatic layers or with significant isothermal layers. Launch days were then declared with the intent of gathering data in selected lapse rate environments. A typical launch day involved tracking three or four pilot balloons. Efforts were made to obtain the longest track possible under existing atmospheric conditions. In conjunction with the pilot balloon tracks, aircraft soundings or balloonsonde³ soundings were obtained.

Track data obtained were reduced by computer to give balloon heights at half-minute intervals during ascent; then height vs time plots were constructed for successive pilot balloon launches. Upon comparison with appropriate soundings, it was decided to choose the commonly encountered dry and moist adiabatic lapse rates for special consideration. Also considered were significant isothermal layers from the surface, and transition zones in going from a dry adiabatic layer or moist adiabatic layer into an isothermal layer aloft.

³ Balloon-borne battery-operated temperature sonde (series 800 MBS) with battery-operated ground receiving and recording station manufactured by COLSPAN Environmental Systems Inc., Boulder, Colo.

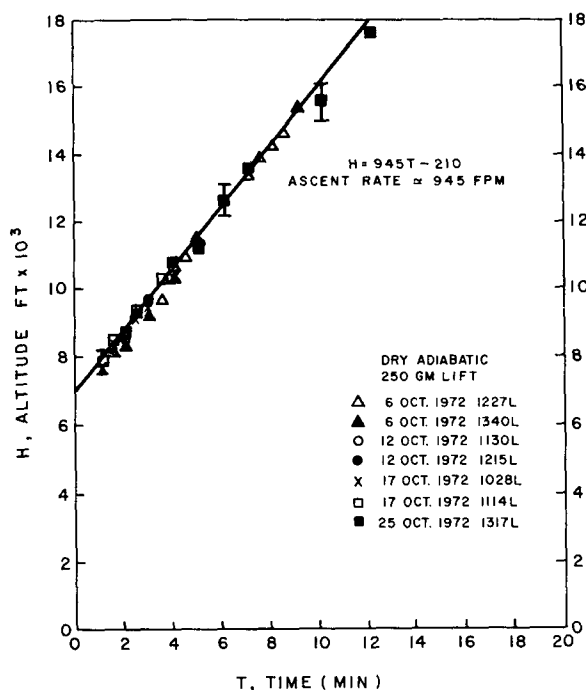


FIG. 3. As in Fig. 2 except for 100-gm (250 gm free-lift) balloons.

3. Results

The NWS assumes a nearly constant ascent rate (NWS form MF5-20)⁴ independent of temperature lapse rate, for 30-gm (139 gm free lift) and 100-gm (449 gm free lift) pilot balloons in the computation of winds aloft. These rates, shown in Fig. 1, are about 600 ft min^{-1} for the 139-gm free lift balloon and 980 ft min^{-1} for the 449-gm free lift balloon as determined from best-fit equations.

The first facet of our investigation of pilot balloon ascent rate variations in different environmental temperature lapse rates was for cases of dry adiabatic environments. Fig. 2 shows the height-time relationship for 30-gm (125 gm free lift) pilot balloons rising from the surface through a dry adiabatic atmosphere. Fig. 3 shows a similar plot for 100-gm (250 gm free lift) pilot balloons rising through a dry adiabatic atmosphere. It can be seen from Figs. 2 and 3 that the ascent rates for both 125- and 250-gm free lift balloons are nearly constant and compare favorably with the "general values" of ascent rates used by the NWS (see Fig. 1).

Next, investigations of the variation of pilot balloon ascent rates in moist adiabatic environments ($-6\text{C km}^{-1} < dT/dZ < -4\text{C km}^{-1}$) were performed. Figs. 4 and 5 show the height-time relationships for 30-gm (125 gm free lift) and 100-gm (250 gm free lift) balloons, respectively, rising from the surface through

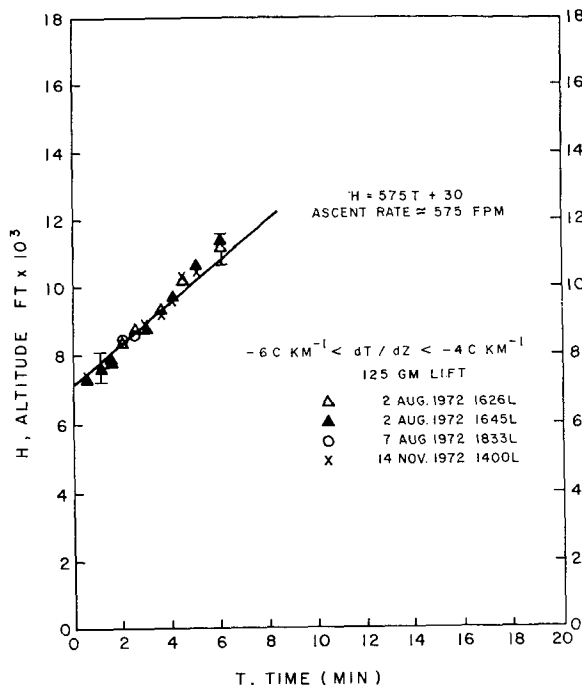


FIG. 4. Composite height vs time plot for 30-gm (125 gm free-lift) balloons rising through a moist adiabatic ($-6\text{C km}^{-1} < dT/dZ < -4\text{C km}^{-1}$) environment from the surface. A best-fit equation is shown with resulting derived balloon ascent rate. Error bars delineate expected accuracy of the measurements.

a moist adiabatic atmosphere. It can be seen from these figures that the ascent rates for both balloons

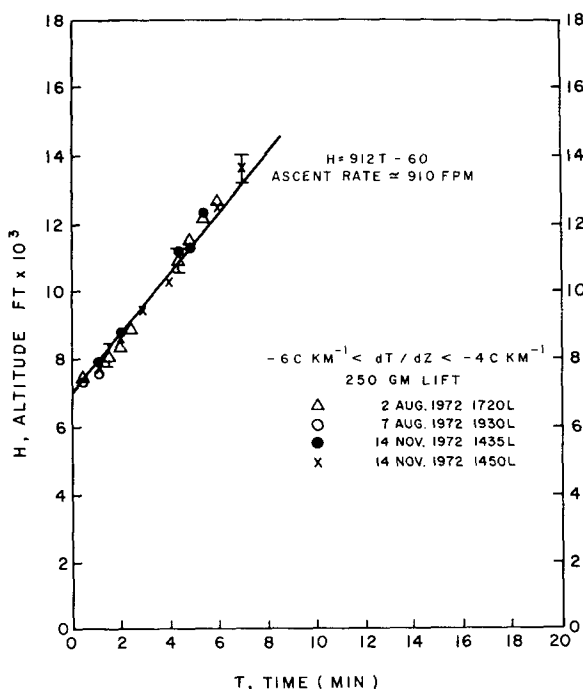


FIG. 5. As in Fig. 4 except for 100-gm (250 gm free-lift) balloons.

⁴ National Weather Service (NOAA) Winds Aloft Computation Sheet (formerly WBAN 20).

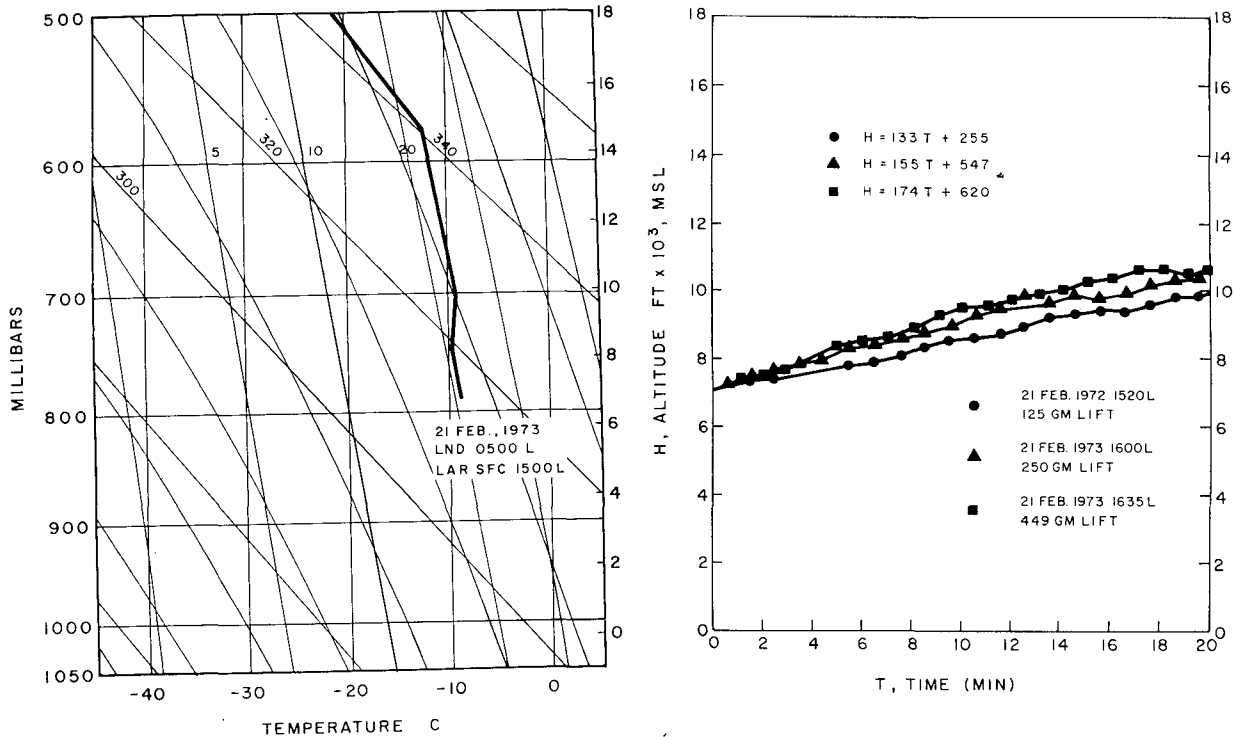


FIG. 6. Plot of the 22 February 1973 Lander, Wyo., 0500 MST rawinsonde observation in conjunction with height vs time plots for a 30-gm (125 gm free-lift) and two 100-gm (250 gm and 449 gm free-lift) pilot balloons. Note that all three pilot balloons remained within the isothermal layer shown for more than 20 min while rising less than 5000 ft.

are nearly constant; however, these ascent rates show a 4 and 7% reduction, respectively, relative to the "general values" of ascent rate used by the NWS.

Our next investigation dealt with the case of an isothermal environment from the surface to about 580 mb as indicated on the 0500 MST Lander, Wyo. (LND), radiosonde observation of 21 February 1973 shown in Fig. 6. The resulting height-time relationships for three balloon weight, free lift combinations [30 gm (125 gm free lift) and 100-gm (250 gm and 449 gm free lift)] show that all three ascent rates for this single case study are nearly constant; moreover, these ascent rates show reductions of 78, 92 and 82%, respectively, relative to the "general values" used by the NWS. For example, a 100-gm (449 gm free lift) pilot balloon is predicted by NWS techniques (see Fig. 2) to be at an altitude of 9800 ft AGL 10 min into the launch. However, as can be seen from Fig. 6, under isothermal conditions, our balloon of identical free lift achieved an altitude of only ~2000 ft AGL.

The acquisition of three very similar height-time profiles for different sized balloons precludes any evidence of balloon rise rate retardation due to leakage or rupture. In addition, the nearly constant rise rate for all three balloon types suggests that rise rate may be independent of balloon size (i.e., free lift) for releases in an isothermal atmosphere.

Finally, since the isothermal atmosphere beginning at the surface was seen to have a deleterious effect on pilot balloon ascent rates, it was decided to investigate what effect a balloon's encounter with an elevated isothermal layer would have on its ascent rate. Fig. 7 is an example of a height-time relationship for a 30-gm (125 gm free lift) and a 100-gm (250 gm free lift) pilot balloon in conjunction with the environmental temperature soundings determined from a Laramie (LAR) based balloonsonde and LND rawinsonde.

The case study cited in Fig. 7 revealed a dry adiabatic layer from the surface capped by an elevated isothermal layer 2500 ft thick. Both the 30-gm and 100-gm pilot balloons were seen to ascend according to the rates shown in Figs. 2 and 3, respectively, within the dry adiabatic layer. However, upon entry into the elevated isothermal layer, the respective ascent rates of both balloons were noticeably retarded.

The ability of various sized pilot balloons to penetrate an elevated isothermal layer was analyzed by determining height-time relationships for pilot balloons after their entry into the elevated isothermal layer. For example, referring to Fig. 7, the 30-gm balloon entered the isothermal layer at the 7th minute near 10,500 ft MSL; the 100-gm balloon entered at the 4th minute. Additional case study data involving

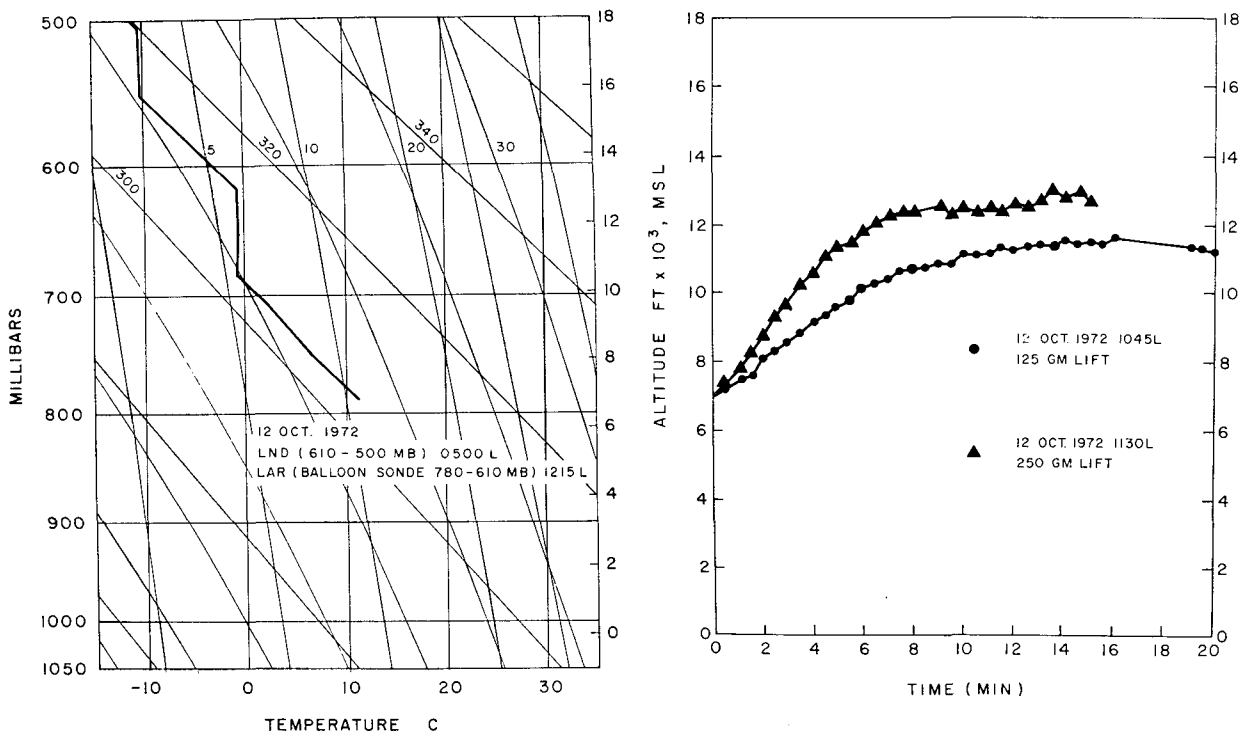


FIG. 7. Plot of the 12 October 1972 composite Lander 0500 MST rawinsonde and Laramie 1215 MST balloonsonde observation in conjunction with height vs time plots for a 30-gm (125 gm free lift) and a 100-gm (250 gm free lift) pilot balloons. Note that both pilot balloons rose at nearly the NWS predicted rates within the dry adiabatic layer but failed to pass through the elevated isothermal layer.

pilot balloon encounters with elevated isothermal layers were also available. Figs. 8a-c show these composite data and a least-squares fit for all three balloon weight, free lift combinations. While a casual inspection of Fig. 8 suggests that a near zero rise rate is attained several minutes after entry into the isothermal layer, a differential analysis of the least-squares fit equation reveals the interesting consequences shown in Table 2. The "maximum penetration depth" of Table 2 may also be interpreted as that height above the base of an isothermal layer above which the pilot balloon will no longer rise. The "time to maximum penetration" is synonymous with the time required for the balloon to approach a zero rise rate according to our data. Thus, balloon penetrations into isothermal layers of depth greater than 2000 ft may seriously hinder the validity of assuming constant rise rates for the entire balloon flight.

4. Summary

Table 3 presents empirical balloon ascent rates and height-time equations for various lapse rate environments and balloon characteristics. The results of Table 3 offer a practical method for height determinations for single-theodolite tracked pilot balloon releases. The appropriate equation for height as a function of time is chosen for the prevailing environment

beginning at the surface. This equation is valid until the balloon enters a new environment; then the equation corresponding to this new environment is used. The actual height of the balloon is now represented by the height achieved in the critical environment plus the height attained in the second prevailing environment. For example, if a 30-gm (125 gm free lift) pilot balloon ascending in a dry adiabatic environment is calculated to reach the base of an isothermal layer after 10 min, then the height above ground at some residence time *T* within the isothermal layer is

$$H = 6186 - 13T^2 + 221T + 5. \tag{1}$$

The validity of (1) rests on knowing that the pilot balloon is within the isothermal layer. Recall from Table 2 that an isothermal layer depth greater than 945 ft (8.5 min residence time) precludes balloon escape through the layer. Therefore, in our example, if the depth of the isothermal layer does not exceed 945 ft (i.e., the residence time *T* is less than 8.5 min), Eq. (1) yields the actual pilot balloon height as it passes through the isothermal layer. If the depth of the isothermal layer exceeds the critical value of 945 ft, the balloon is captured within the isothermal layer and attains the limiting constant height of $H = 6186 + 945 = 7131$ ft.

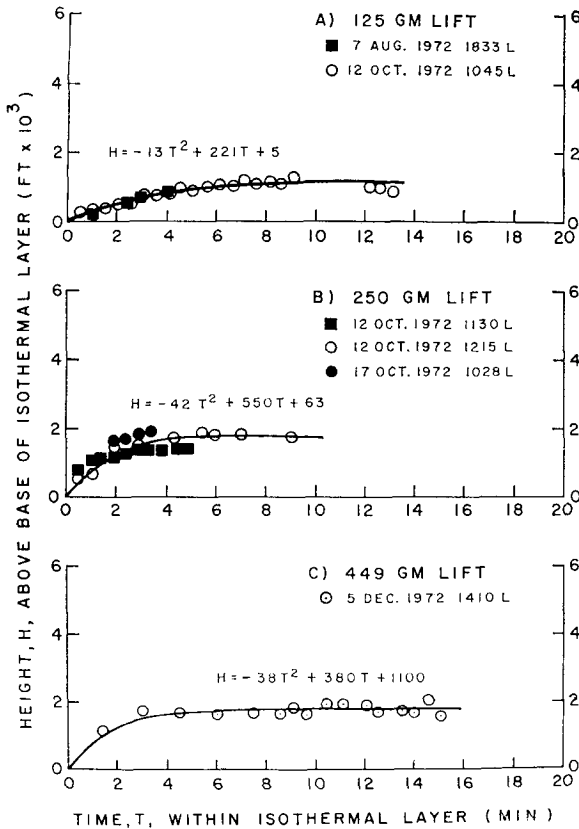


FIG. 8. Composite height vs time plots for balloons rising into an elevated isothermal layer. A best-fit equation is shown for H (height above isothermal layer base) versus T (time within the isothermal layer): (a) 30 gm (125 gm free lift), (b) 100 gm (250 gm free lift), (c) 100 gm (449 gm free lift).

Sinha (1959) states that the pilot balloon ascent rate V may be expressed in the form

$$V^2 = Fg / (\rho d^2 \kappa), \tag{2}$$

TABLE 3. Pibal ascent rates and height-vs-time relationships in various temperature lapse rate environments for various balloon sizes and free lifts, where H is the height (ft) above the base of the prevailing temperature lapse rate environment and T the residence time (min) within this temperature lapse rate environment.

Balloon size (gm)	Free lift (gm)	Environment	Ascent rate dH/dT (ft min ⁻¹)	Empirical equation H vs T	Number of ascents
30	139*	not specified	600	$H = 600T + 5$	NWS assumed values
30	125	dry adiabatic	617	$H = 617T + 16$	10
30	125	moist adiabatic	575	$H = 575T + 30$	47
30	125	isothermal	133	$H = 133T + 255$	5
30	125	isothermal from dry/moist adiabatic	-0.64H+600	$H = -13T^2 + 221T + 5$	2
100	250	dry adiabatic	945	$H = 945T - 210$	12
100	250	moist adiabatic	912	$H = 912T - 60$	47
100	250	isothermal	155	$H = 155T + 547$	3
100	250	isothermal from dry/moist adiabatic	-0.6 H+950	$H = -42T^2 + 530T + 63$	4
100	449*	not specified	980	$H = 980T + 5$	NWS assumed values
100	449*	isothermal	174	$H = 174T + 620$	32
100	449*	isothermal from dry/moist adiabatic	-0.5 H+1000	$H = -38T^2 + 380T + 1100$	3

* Values used by the National Weather Service.

TABLE 2. The maximum penetration depth and time to maximum penetration within elevated isothermal layers as a function of balloon size and free lift.

Size (gm)	Free lift (gm)	Maximum penetration depth (ft)	Time to maximum penetration (min)
30	125	945	8.5
100	250	1670	5.2
100	449	2000	5.0

where F is the free lift weight of the balloon, g the acceleration of gravity, ρ air density, d the balloon diameter, and κ the coefficient of aerodynamic resistance. Using the ideal gas law $P/\rho = R_d T^*$ and the hydrostatic equation $\partial P/\partial z = -\rho g$, where P is air pressure, R_d the gas constant for dry air, and T^* the virtual temperature, one obtains

$$dP/dz = -gP / (R_d T^*), \tag{3}$$

after substitution for ρ in the hydrostatic equation. In an atmosphere possessing a constant temperature lapse rate ($dT^*/dz = \Gamma$) virtual temperature is a function of height ($T^* = \Gamma z + \text{constant}$). Assuming the surface virtual temperature to be 300K, we have

$$T^* = \Gamma z + 300. \tag{4}$$

Substituting in (3) yields

$$dP/dz = -gP / [R_d (\Gamma z + 300)]. \tag{5}$$

Upon integration Eq. (5) becomes

$$P = (\Gamma z + 300)^{-g/(R_d \Gamma)} \exp(\text{constant}). \tag{6}$$

Evaluating the constant of integration at $P(0) = 1013$ mb yields

$$P = 2.166 \times 10^{-6} (\Gamma z + 300)^{-g/R_d \Gamma}. \tag{7}$$

Upon substitution for P from (7) the ideal gas law becomes

$$\rho = P/R_d T^* = 2.166 \times 10^{-6} (\Gamma z + 300)^{-g/R_d \Gamma} / (R_d T^*). \quad (8)$$

Then, using (8) to substitute for ρ in (2), we have

$$V^2 = F g R_d T^* / [2.166 \times 10^{-6} (\Gamma z + 300)^{-g/R_d \Gamma} d^2 \kappa]. \quad (9)$$

From Eq. 9 one sees that balloon ascent rate is a function of virtual temperature, lapse rate, altitude and balloon diameter in any constant temperature lapse rate environment. Temperature typically decreases with height and balloon diameter increases during the balloon's ascent. These two variables typically decrease the balloon ascent rate described in (9). The effect of increasing altitude is to increase balloon ascent rate under constant temperature lapse rate conditions. Thus, an overall balance of forces affecting balloon ascent rate under normal atmospheric conditions is possible.

If temperature lapse rate were constant but smaller in magnitude than the dry adiabatic lapse rate, Eq. (9) shows that the balloon ascent rate would be expected to decrease accordingly. Also, the increase in balloon ascent rate attributed to Γz variations would be less than the dry adiabatic case.

If temperature lapse rate became zero ($\Gamma=0$), i.e., the balloon entered an isothermal layer, Eq. (9) predicts that the balloon ascent rate would approach zero.

Thus, the results delineated in this work are predicted by Eq. (9) in the case of constant lapse rate environments or isothermal layers. The observational evidence contained in this paper concerning the effect of tropospheric temperature lapse rates on the ascent rates of pilot balloons may have a bearing on the

interpretations given to analyzed wind data gleaned from single theodolite systems. The assumption of "general value" pilot balloon ascent rates when balloons are within isothermal layers may result in a fictitious wind speed maximum within the isothermal layer. It appears essential that environmental temperature lapse rates, especially isothermal ones, be monitored closely in order to avoid questionable interpretations due to the assumption of uniform "general value" ascent rates for meteorological balloons.

Acknowledgments. This research was made possible by the Environmental Protection Agency under Grant R-800875 to the Department of Atmospheric Resources, College of Engineering, University of Wyoming. Appreciation is expressed to my colleagues at the University of Wyoming for their help in acquiring the data.

REFERENCES

- Baynton, H. W., 1968: Stability inferences from precision rawins. *Mon. Wea. Rev.*, **96**, 47-56.
- Butler, R., and L. D. Duncan, 1968: Empirical estimates of errors in double-theodolite wind measurements. Ecom-5178, DA Task IT014501B53A-10, U. S. Army Electronics Command, White Sands Missile Range, N. M. 13 pp.
- Reynolds, R. D., 1966: The effect of atmospheric lapse rates on balloon ascent rates. *J. Appl. Meteor.*, **5**, 537-541.
- Rider, L. J., and A. J. Armendariz, 1970: Vertical wind component estimates up to 1.2 km above ground. *J. Appl. Meteor.*, **9**, 64-71.
- Sinha, K. L., 1959: Evaluation of the constant of the balloon-ascent formula at different Reynolds numbers from the value of the coefficient of aerodynamic resistance. *J. Meteor.*, **16**, 692-693.
- U. S. Weather Bureau, 1942: Instructions for making pilot balloon observations. Circular O, Weather Bureau Manual No. 1278, Govt. Printing Office, Washington, D. C., 65 pp.